

A MODEL OF OPPOSED-FLOW FLAME SPREAD OVER CHARRING MATERIALS

ARVIND ATREYA¹ AND HOWARD R. BAUM²

¹*Department of Mechanical Engineering
University of Michigan
Ann Arbor, MI 48109, USA*

²*National Institute of Standards and Technology
Building and Fire Research Laboratory
Gaithersburg, MD 20899, USA*

This paper presents a theoretical description of a diffusion flame spreading against the wind on a semi-infinite charring solid. It extends the previous flame spread models on “vaporizing” solids to charring materials like wood and provides a realistic description of the gas phase. To make the problem analytically tractable, a mixture fraction approach is used in the gas phase and the no-slip boundary condition is satisfied only for $x > 0$. In the solid phase, the charring solid is assumed to decompose abruptly (endothermically or exothermically) into char and fuel gases at a specified pyrolysis temperature. The steady-state coupled elliptic equations for conservation of energy, mixture fraction, and momentum in the gas phase and conservation of energy in the char and the pristine solid are solved by using orthogonal parabolic coordinates. A general analytical solution is presented that reduces to de Ris’s flame spread formula in the limit of zero char thickness and with similar assumptions. The growing char layer in the solid phase has considerable influence on the flame spread rate. It is seen that formation of a thicker char layer significantly retards the spread rate. Unique steady-state solutions for the parabolic char-material interface were found to exist only for Stefan number > -1 . For Stefan number $= -1$ (i.e., exothermic), two solutions were found. One of these solutions corresponds to the location of the char-solid interface at infinity, indicating the likelihood of a thermal runaway. This happens regardless of the property values.

Introduction

Opposed-flow flame spread over the surface of a semi-infinite solid has been a subject of much investigation in the past. Several elegant analytical flame spread models have also appeared in the literature [1–4]. It is indeed fascinating to note how the authors of these studies reduced the complex flame spread problem with novel approximations to obtain analytical flame spread formulas. It is even more fascinating to see how well these formulas agree with the experimental measurements for materials for which they were designed. Previous studies, however, have focused primarily on the gas-phase part of the problem, and the solid was assumed to “vaporize” at a known fixed temperature. Yet, a large number of natural and synthetic polymers do not simply vaporize; instead, they undergo a complex thermal decomposition process which results in an insulating layer of char on the surface. This char layer thickens with time and gives rise to a two-phase moving-boundary problem in the solid. Due to this difficulty, an understanding of flame spread over these solids and the role played by the char layer is lacking. To obtain an analytical solution, it was also necessary to simplify the gas-phase momentum and

continuity equations by using a uniform Oseen velocity U_g and the constant pressure condition. Thus, the objectives of the present study are (1) to extend the previous work on vaporizing solids to charring materials like wood and (2) to provide a realistic description of the gas phase.

The analyses most relevant to the present problem are those of de Ris [1] and Wichman and Williams [3]. De Ris, in his seminal work on opposed-flow flame spread [1], used the Oseen approximation in the gas phase, and by assuming infinite reaction rates, he developed a flame spread formula relating the flame spread rate to the solid and gas-phase properties, which were assumed constant. His results indicate that due to the approximations made in the gas phase, the flame sheet almost lies along the fuel surface behind the flame-inception point.

Wichman and Williams [3] have also employed the Oseen approximation in the gas phase and have utilized de Ris’s result [1] by hypothesizing at the outset that the combustion heat release occurs along the fuel surface. This hypothesis eliminates the necessity of considering the gas-phase species conservation equations and thus allows a more detailed analysis of a simplified thermal model. Their model also yields the same formula for the opposed-flow flame

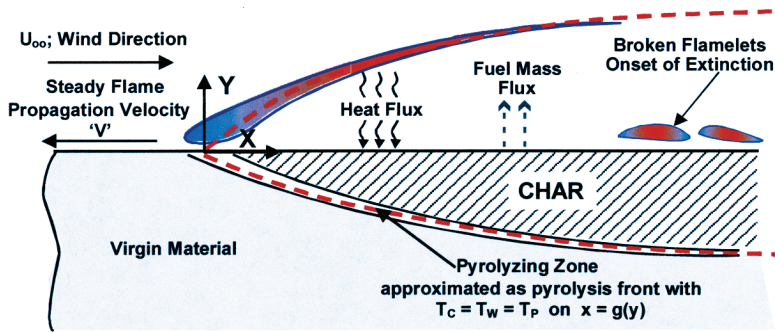


FIG. 1. Schematic of the physical problem: steady propagation of an opposed-flow diffusion flame on the surface of a charring solid. Dotted lines show the approximations made in the gas and solid phases. The pyrolysis zone is approximated by a pyrolysis front and the reaction zone by a flame sheet.

spread rate as de Ris's model. Their formula was derived by requiring that a steady spread rate must be sufficient to remove the combustion heat release by downstream gas- and solid-phase convection (in the flame-fixed coordinates). Later, Atreya [5,6] showed that to obtain de Ris's formula, it was also unnecessary to consider heat transfer between the gas and the solid phases upstream of the flame front. This critical observation enabled the use of parabolic coordinates that simplified the analysis. These concepts for determining the steady flame spread rate are exploited here to extend the theory of opposed-flow flame spread to charring materials. In addition, the Oseen approximation is eliminated and a realistic description of the gas-phase flame is provided in terms of a mixture fraction for a variable-density gas. The coupled elliptic equations in the three media, gas, char, and virgin material, are analytically solved to obtain the flame spread rate.

Model Formulation

The physical problem considered here is schematically shown in Fig. 1. In the model problem, the slab is assumed to be semi-infinite and the diffusion flame is assumed to extend to infinity downstream of the flame-inception point (as shown by the dotted line in Fig. 1 in the plane $y > 0$, the flame sheet). In the real case, the thickening of the char layer and reradiation from the char surface will result in extinction of the diffusion flame further downstream of the flame-inception point. This aspect, caused by finite reaction rates, is ignored. The origin of the coordinate system is located at the flame-inception point, and the flame is held stationary by feeding the solid into the flame at the steady flame spread rate V . As the solid travels into the flaming zone, it decomposes abruptly (endothermically or exothermically) at a specified pyrolysis temperature T_p , resulting in a pyrolysis surface (as shown by the dotted line in Fig. 1 in the plane $y < 0$). Again, in reality, a

pyrolysis zone is formed where thermal decomposition occurs over a region of finite thickness. However, this is ignored in the simplified model presented here.

A further simplification is made based on the previous results [5,6] that show that the heat exchange between the solid and the gas across the plane $y = 0$ and $x < 0$ is small. Data for wood [7] shows that the total heat exchanged across the plane $y = 0$ and $x < 0$ is less than 15% of the heat conducted through the solid across the plane $x = 0$ and $y < 0$. Physically, in the region $x < 0$, with both the solid and the gas initially at T_∞ , significant heat exchange between the two media does not occur until they reach close to the flame-inception point. For high gas velocities, additional heat is transferred to the gas in the region $x < 0$ via upstream conduction of heat through the solid and vice versa. Thus, most of the heat conducted upstream across $x = 0$ in both the solid and the gas phases remains within the respective phases. This is an important observation because the temperature gradient in both phases can now be approximated by zero on $x < 0$ and $y = 0$. This enables the use of parabolic coordinates both in the solid and the gas phases. Parabolic coordinates automatically satisfy the zero gradient boundary condition on $x < 0$ and $y = 0$. As will be seen later, de Ris's flame spread formula [1] is recovered in the limit of zero char thickness by this analysis, implying that in the classical solution by de Ris, the Oseen flow assumption, in effect, rendered the heat exchange between the two phases along $y = 0$ and $x < 0$ irrelevant to determining the flame spread rate.

Gas Phase

The conservation of mass, gaseous species, and energy are described by the following equations:

$$\frac{\partial}{\partial x}(\rho u) + \frac{\partial}{\partial y}(\rho v) = 0 \quad (1)$$

$$\rho u \frac{\partial Z}{\partial x} + \rho v \frac{\partial Z}{\partial y} = \frac{\partial}{\partial x} \left(\rho D \frac{\partial Z}{\partial x} \right) + \frac{\partial}{\partial y} \left(\rho D \frac{\partial Z}{\partial y} \right) \quad (2)$$

where $\rho(x, y)$ is the gas density and $Z(x, y)$ is the mixture fraction in a two-dimensional flow field $\bar{u} = (u, v)$. All scalar variables are assumed to be related uniquely to the mixture fraction. The mass conservation equation (equation 1) can be satisfied exactly with the introduction of a stream function $\psi(x, y)$ defined as $\partial\psi/\partial y = \rho u$ and $\partial\psi/\partial x = -\rho v$.

These equations are transformed by introducing dimensionless parabolic coordinates defined by the expression

$$\zeta + i\eta = \sqrt{\frac{U_\infty}{v_\infty}} (x + iy) \quad (3)$$

Here, U_∞ is the ambient wind speed in a coordinate system moving with the flame front, and v_∞ is the kinematic viscosity evaluated at ambient temperature. By defining a Howarth transformed variable, $\zeta = \int_0^\eta (\rho(\eta)/\rho_\infty) d\eta$, postulating $\psi = \mu_\infty \zeta f(\zeta)$, and seeking solutions of the form $Z = Z(\zeta)$, equation 2 can be reduced to

$$f(\zeta) \frac{dZ}{d\zeta} + \frac{1}{Sc} \frac{d}{d\zeta} \left(\frac{\rho(Z)}{\rho_\infty} \frac{D(Z)}{D_\infty} \frac{dZ}{d\zeta} \right) = 0 \quad (4)$$

Here, $Sc = v_\infty/D_\infty$ is the Schmidt number. The assumption that all scalar variables are functions of Z implies that the Lewis number is unity. Thus, $Sc = Pr = \mu C_p/\lambda$.

The boundary conditions for physical variables such as temperature (T , or sensible enthalpy h^S), fuel and oxidizer mass fractions (Y_F and Y_O), and velocities are as follows. Char-gas interface:

$$\begin{aligned} \zeta = 0; y = 0; x \geq 0: T = T_S; h^S = h_0^S; \\ Y_F = Y_{F,0}; Y_O = 0, \text{ and } u = 0 \end{aligned} \quad (5)$$

Far from the burning surface, ambient conditions exist:

$$\begin{aligned} \zeta \rightarrow \infty; \eta \rightarrow \infty; y \rightarrow \infty: T = T_\infty; h^S = h_\infty^S; \\ Y_F = 0; Y_O = Y_{O,\infty}, \text{ and } u = U_\infty \end{aligned} \quad (6)$$

The algebraic state relations are constructed such that $Z(0) = 1$ and $\lim_{\zeta \rightarrow \infty} Z(\zeta) = 0$. Since Z depends only on ζ , any physical quantity related to Z by state relations will satisfy the zero normal gradient boundary condition for $x \leq 0$. The gas-phase problem in the burning region is essentially reduced to the problem solved by Emmons [8] because for $x \gg y$, that is, inside the boundary layer, the parabolic coordinates reduce to

$$\xi = \sqrt{\frac{U_\infty x}{v_\infty}} \text{ and } \zeta = \frac{1}{2} \sqrt{\frac{U_\infty}{v_\infty x}} \int_0^y \frac{\rho(\tilde{z})}{\rho_\infty} dy \quad (7)$$

Upstream of the burning region, the no-slip condition is violated, but the upstream influence of the

variable density flow is retained. In the boundary layer region, the x -momentum equation takes the approximate form:

$$\rho \left(u \frac{\partial u}{\partial x} + v \frac{\partial u}{\partial y} \right) = \frac{\partial}{\partial y} \left(\mu \frac{\partial u}{\partial y} \right) \quad (8)$$

Choosing $f(\zeta)$ as the solution of equation 8, we have

$$f(\zeta) f''(\zeta) + \frac{d}{d\zeta} \left(\frac{\rho \mu}{\rho_\infty \mu_\infty} f''(\zeta) \right) = 0 \quad (9)$$

Boundary conditions require that at the burning surface $u = 0$, but the normal component of the velocity v (the blowing velocity) must correspond to that supplied by the solid-phase solution. Far from the burning surface, $u = U_\infty$. In terms of $f(\zeta)$, these conditions reduce to

$$f(0) = -m \quad f'(0) = 0 \quad \lim_{\zeta \rightarrow \infty} f'(\zeta) = 2 \quad (10)$$

Here, m is the dimensionless parameter that describes the magnitude of the blowing velocity. It has to be determined by the solid-phase solution. It is important to note that while the burning zone problem essentially reduces to the Emmons [8] problem, the velocity field is valid everywhere. Moreover, the solution is exact far from the burning surface because the asymptotic form of the solution for ψ is an irrotational flow which exactly satisfies the constant property Navier-Stokes equations. The asymptotic solution for the stream function is $\psi = 2\mu_\infty \xi(\eta - c)$.

The gas-phase problem is reduced to the solution of two ordinary differential equations (ODEs). The effect of the solid phase is felt only through the blowing parameter m , the Schmidt number Sc , and the state relations. Thus, within unknown values of m and Sc , the gas-phase solution can be obtained. The analysis is greatly simplified by assuming the temperature dependence of viscosity and diffusivity are such that $\rho \mu = \rho_\infty \mu_\infty$ and $\rho^2 D = \rho_\infty^2 D_\infty$. Thus, the governing equations become

$$f'''(\zeta) + f(\zeta) f''(\zeta) = 0 \quad (11)$$

$$Z''(\zeta) + Sc f(\zeta) Z'(\zeta) = 0 \quad (12)$$

The solution for Z that satisfies the boundary conditions is readily found to be

$$\begin{aligned} Z(\zeta, Sc) = 1 - g(\zeta, Sc)/g(\infty, Sc) \\ \text{where } g(\zeta, Sc) = \int_0^\zeta [f''(t)]^{Sc} dt \end{aligned} \quad (13)$$

The problem is now reduced to the solution of the Blasius equation (equation 11) with boundary conditions given by equation 10. Once Z is known, all other scalar variables are found by appropriate state relations as follows:

$$\begin{aligned} Z(\zeta) &= \frac{[h^S(\zeta) - h_{\infty}^S - Q_O(Y_{O,\infty} - Y_O(\zeta))]}{[h_0^S - h_{\infty}^S - Q_O Y_{O,\infty}]} \\ &= \frac{SY_F(\zeta) - (Y_O(\zeta) - Y_{O,\infty})}{SY_{F,0} + Y_{O,\infty}} \end{aligned} \quad (14)$$

Using the fact that Y_O is zero on the fuel side of a diffusion flame and Y_F is zero on the oxidizer side, $h^S(\zeta)$, $Y_F(\zeta)$, and $Y_O(\zeta)$ may be found from the knowledge of $Z(\zeta)$. Also, $Z(\zeta_{fl})$ may be found by requiring that both Y_F and Y_O are zero at the flame surface. Finally, using the approximate equation of state $\rho h^S = \rho_{\infty} h_{\infty}^S = \text{const.}$, we retrieve the parabolic coordinate η from ζ by the relation $\eta = \int_0^{\zeta} (\rho_{\infty} / \rho(t)) dt$.

On the fuel side ($Z \geq Z_{fl}$),

$$\frac{h^S}{h_{\infty}^S} = \frac{\rho_{\infty}}{\rho} = (1 + E) + Z(\zeta) \left[\frac{h_0^S}{h_{\infty}^S} - E - 1 \right] \quad (15)$$

Here, h^S is the sensible enthalpy, and the subscript 0 indicates the fuel surface. Also, $E = (Q_O Y_{O,\infty} / h_{\infty}^S)$ and Q_O is the heat of reaction per unit mass of O_2 consumed. Thus,

$$\eta = \zeta(1 + E) + \left[\frac{h_0^S}{h_{\infty}^S} - E - 1 \right] \int_0^{\zeta} Z(\zeta) d\zeta \quad (16)$$

On the oxidizer side ($0 \leq Z \leq Z_{fl}$),

$$\frac{h^S}{h_{\infty}^S} = \frac{\rho_{\infty}}{\rho} = 1 + Z(\zeta) \left[\frac{h_0^S}{h_{\infty}^S} - 1 + E \left(\frac{SY_{F,0}}{Y_{O,\infty}} \right) \right] \quad (17)$$

where $S = (v_O M_O) / (v_F M_F)$ and $Y_{F,0}$ are the stoichiometric oxidizer to fuel ratio by mass and the mass fraction of fuel at the surface. Thus,

$$\eta = \zeta + \left[\frac{h_0^S}{h_{\infty}^S} - 1 + E \left(\frac{SY_{F,0}}{Y_{O,\infty}} \right) \right] \int_0^{\zeta} Z(\zeta) d\zeta \quad (18)$$

Solid Phase

Equations for energy transfer in the pristine solid and char (denoted by subscripts "w" and "c," respectively) are needed to describe the solid-phase part of the flame spread problem depicted in Fig. 1. Constant thermophysical properties are assumed, and regression or oxidation of the char surface is ignored. This leads to the following set of steady-state equations for the temperature field in the two media. For the pristine solid:

$$\begin{aligned} \rho_w VC_{pw} \frac{\partial T_w}{\partial x} - \lambda_w \left(\frac{\partial^2 T_w}{\partial x^2} + \frac{\partial^2 T_w}{\partial y^2} \right) &= 0 \\ -\infty < x \leq g(y); y &\leq 0 \end{aligned} \quad (19)$$

for the char matrix:

$$\begin{aligned} \rho_c VC_{pc} \frac{\partial T_c}{\partial x} - \lambda_c \left(\frac{\partial^2 T_c}{\partial x^2} + \frac{\partial^2 T_c}{\partial y^2} \right) &= 0 \\ g(y) \leq x \leq \infty; y &\leq 0 \end{aligned} \quad (20)$$

Appropriate boundary conditions require that along the interfaces the temperatures are equal. At the char-gas interface, the temperature is assumed to be a constant, that is, $T_g(x, 0) = T_c(x, 0) = T_s$ for $x > 0$, and the boundary conditions along $x < 0$ are

$$\begin{aligned} T_w(x, 0) &= T_g(x, 0) \text{ and} \\ \lambda_g \frac{\partial T_g}{\partial y}(x, 0) &= \lambda_w \frac{\partial T_w}{\partial y}(x, 0) = 0 \text{ for } x < 0 \end{aligned} \quad (21)$$

Far from the interface, the boundary conditions are

$$\begin{aligned} T_g(-\infty, y) &= T_g(x, \infty) = T_{\infty} & T_g(\infty, y) &\text{ is bounded} \\ T_w(-\infty, y) &= T_w(x, -\infty) = T_{\infty} & T_c(\infty, y) &\text{ is bounded} \end{aligned} \quad (22)$$

The location of the char-material interface (referred to as $x = g(y)$ in Fig. 1) is not *a priori* known and will be obtained as part of the solution. At this interface, the pristine solid is assumed to abruptly decompose (endothermically or exothermically) into char and fuel gases at a specified pyrolysis temperature T_p . Thus, $T_w[g(y), y] = T_c[g(y), y] = T_p$. The final condition is obtained by energy balance at the isothermal boundary between char and the solid (represented by $f(x, y) = \text{const.}$) as it moves with the steady flame spread velocity V :

$$\begin{aligned} \lambda_c \sqrt{\left(\frac{\partial T_c}{\partial x} \right)^2 + \left(\frac{\partial T_c}{\partial y} \right)^2} &= \lambda_w \sqrt{\left(\frac{\partial T_w}{\partial x} \right)^2 + \left(\frac{\partial T_w}{\partial y} \right)^2} \\ &+ Q \rho_w V \left(\frac{\partial f}{\partial x} \right) / \sqrt{\left(\frac{\partial f}{\partial x} \right)^2 + \left(\frac{\partial f}{\partial y} \right)^2} \end{aligned} \quad (23)$$

Here, Q is the amount of heat liberated or absorbed at the interface per unit mass of pristine solid, being positive when endothermic.

The solid-phase equations and boundary conditions again lend themselves to the use of parabolic coordinates defined by the relation

$$\beta + i\omega = \sqrt{\frac{2V}{\alpha_w}} (x + iy) \quad (24)$$

where V is the flame speed and $\alpha_w = (\lambda_w / \rho_w C_{pw})$. Again, solution of the form $T = T(\omega)$ satisfies all the equations and boundary conditions in the solid phase. Normalizing temperature by the relations

$$\begin{aligned} \theta_g &= (T_g - T_{\infty}) / (T_s - T_{\infty}) \\ \theta_w &= (T_w - T_{\infty}) / (T_s - T_{\infty}) \\ \theta_c &= (T_c - T_{\infty}) / (T_s - T_{\infty}) \\ \theta_p &= (T_p - T_{\infty}) / (T_s - T_{\infty}) \end{aligned} \quad (25)$$

and rewriting equations 19–23 in terms of parabolic

coordinates after assuming $\theta = \theta(\omega)$, we obtain two ODEs that can be solved to yield

$$\begin{aligned}\theta_w &= \theta_p \operatorname{erfc}\left(\frac{\omega}{\sqrt{2}}\right) / \operatorname{erfc}\left(\frac{c}{\sqrt{2}}\right) \text{ and} \\ \theta_c &= 1 - (1 - \theta_p) \operatorname{erf}\left(\frac{\sqrt{\delta_c}}{\sqrt{2}} \omega\right) / \operatorname{erf}\left(\frac{\sqrt{\delta_c}}{\sqrt{2}} c\right)\end{aligned}\quad (26)$$

where the value of c , which defines the parabolic char-solid interface, is obtained from the transcendental equation:

$$\begin{aligned}\left\{\bar{\lambda} \frac{(1 - \theta_p)}{\theta_p} \sqrt{\delta_c}\right\} \left\{\frac{\exp\left(-\frac{c^2 \delta_c}{2}\right)}{\operatorname{erf}\left(\frac{\sqrt{\delta_c}}{\sqrt{2}} c\right)}\right\} - \frac{\exp\left(\frac{c^2}{2}\right)}{\operatorname{erfc}\left(\frac{c}{\sqrt{2}}\right)} \\ = \bar{Q} \sqrt{\frac{\pi}{2}} c\end{aligned}\quad (27)$$

In the limit as $c \rightarrow 0$ (i.e., the char layer becomes very thin), equation 27 indicates the physically obvious result, that is, $\theta_p \rightarrow 1$. Thus, for $c = 0$, $\theta_c = \theta_p = 1$. In equations 26 and 27,

$$\delta_c = \left[\left(\frac{\lambda_w}{\rho_w C_{pw}} \right) / \left(\frac{\lambda_c}{\rho_c C_{pc}} \right) \right]$$

is the ratio of pristine solid to char thermal diffusivities and $\bar{\lambda} = (\lambda_c / \lambda_w)$ is the ratio of char to pristine solid conductivities. Also, $\bar{Q} = Q / C_{pw}(T_p - T_\infty)$ is the ratio of heat required to decompose a unit mass of pristine solid to the heat required to bring this unit mass from ambient to the pyrolysis temperature. It is the Stefan number.

Flame Spread Rate

The steady flame spread rate is determined by two physical conditions that have not yet been satisfied. These are (1) The energy balance downstream of the point of flame inception. Mathematically, this condition along the burning surface ($y = 0; x \geq 0$) states

$$-\lambda_g \frac{\partial T_g}{\partial y}(x, 0) = -\lambda_c \frac{\partial T_c}{\partial y}(x, 0) \quad (28)$$

(2) The second condition corresponds to the evolution of the fuel mass from the solid. This condition, determined from the solid-phase solution, yields the “blowing parameter” m . Note that the pyrolysis products are produced as the char-solid interface (defined by the parabola $\omega = c$) travels through the solid at a constant velocity V converting the pristine solid to char and generating a mass proportional to $(\rho_w - \rho_c)$. After appropriate vector manipulation, this condition yields $(\rho v)_{@y=0} = (\rho_w -$

$\rho_c)c\sqrt{\alpha_w V/2x}$. Equating this to $-(\partial\psi/\partial x)_{@y=0}$, we obtain an expression for m as

$$f(0) = -m = -\sqrt{\frac{2\alpha_w V}{v_\infty U_\infty}} \frac{(\rho_w - \rho_c)}{\rho_{\infty, \text{gas}}} c \quad (29)$$

Utilizing $h^S(\zeta)$ from equation 14 after setting $Y_O = 0$ for the fuel side, we can obtain the temperature gradient in the gas phase adjacent to the char surface. Likewise, the temperature gradient in the char is obtained from equation 26. Substituting these in equation 28 yields

$$\begin{aligned}\left(\frac{\mu_0 \rho_0}{\mu_\infty \rho_\infty}\right) (h_0^s - h_\infty^s - Q_0 Y_{0\infty}) \frac{[f''(0, m)]^{Sc}}{Sc \cdot m \cdot g(\infty, Sc, m)} \\ = \sqrt{\frac{2\lambda_c \rho_c C_{pc}}{\pi \lambda_w \rho_w C_{pw}}} \left(\frac{\rho_w}{\rho_w - \rho_c}\right) \frac{C_{pw}(T_s - T_p)}{c \cdot \operatorname{erf}\left(\frac{\sqrt{\delta_c}}{\sqrt{2}} c\right)}\end{aligned}\quad (30)$$

Here, $f''(0, m)$ is numerically determined from the Blasius solution for prescribed values of m and Sc . As seen from equation 27, c —the parabolic char-solid interface—depends entirely on the solid-phase material properties. Thus, equation 30 determines an appropriate value of m that satisfies the energy balance at the burning surface. Once m is determined, equation 29 is used to determine the flame spread rate. Throughout this analysis, U_∞ is taken as the gas velocity relative to a stationary flame. Thus, for a flame moving at velocity V , the actual U_g is equal to $(U_\infty + V)$. Using this, equation 29 yields the flame spread formula in terms of m :

$$\left(\frac{V}{U_\infty}\right) = \left[\left(\frac{c}{m}\right)^2 \left(\frac{\rho_w - \rho_c}{\rho_{\infty, \text{gas}}}\right)^2 \frac{2\alpha_w}{v_\infty} - 1 \right]^{-1} \quad (31)$$

For the special case of Oseen flow (and imposing the assumptions of Refs. [1,3,5,6]), this analysis yields the flame spread rate as

$$\left(\frac{V}{U_\infty}\right) = \frac{\lambda_g \rho_g C_{pg}}{\lambda_c \rho_c C_{pc}} \left[\left(\frac{T_f - T_s}{T_s - T_p}\right) \operatorname{erf}\left(\sqrt{\frac{\delta_c}{2}} c\right) \right]^2 \quad (32)$$

It is interesting to note that in the limit of zero char thickness (i.e., as $c \rightarrow 0$ and $T_p \rightarrow T_s$), a “vaporizing” solid is obtained. In this limit, equation 32 reduces to de Ris’s spread formula [1].

Discussion and Conclusions

Char-Material Interface

The char-material interface is defined by the parabola $\omega = c$, where the value of c is obtained from the solution of the transcendental equation (equation 27). In equation 27, \bar{Q} is the Stefan number (positive for endothermic decomposition) and the terms from left to right can be shown to be as (1)

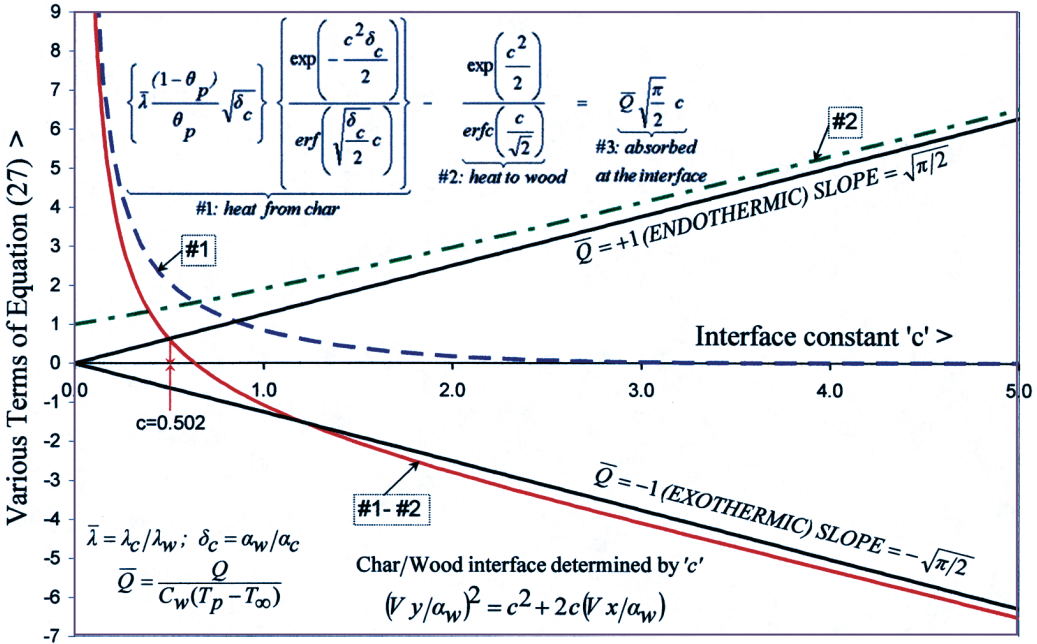


FIG. 2. Graphical determination of the value of the charring constant c that determines the parabolic char-material interface described by equation 27.

the heat flux (non-dimensional) to the interface from char (goes to 0 as $c \rightarrow \infty$ and goes to ∞ as c tends to 0); (2) the heat flux (non-dimensional) leaving the interface into the pristine solid (goes to 1 as c goes to 0 and goes to ∞ like $\sqrt{\pi/2}$ as c tends to ∞); and (3) the heat absorbed or liberated at the char-pristine solid interface (on the right-hand side of equation 27). The solution requires four input parameters: $\bar{\lambda}$, \bar{Q} , δ_c , and θ_p . For representative values of these parameters ($\bar{\lambda} = 1/3$, $\theta_p = 0.275$, and $\delta_c = 0.75$), various terms of the transcendental equation 27 are plotted in Fig. 2. The value of c is determined by the intersection of the straight line representing the right-hand side of equation 27 and the composite curve representing the left-hand side of equation 27. The slope of the straight line is proportional to the Stefan number \bar{Q} . It is interesting to note that a steady-state solution presented here exists only for $\bar{Q} > -1$. At $\bar{Q} = -1$ (exothermic), the intersection occurs at a finite value of c as well as at infinity, indicating the likelihood of a thermal runaway. This happens for any set of values of $\bar{\lambda}$, δ_c , and θ_p , because as $c \rightarrow \infty$, the second term on the left-hand side of equation 27 tends to ∞ like $\sqrt{\pi/2} c$ and the first term goes to zero. Thus, the left-hand side of equation 27 is asymptotic to a straight line with slope $-\sqrt{\pi/2}$ and passing through the origin. Since such a thermal runaway has not been observed for a charring material like wood, the maximum exothermic value for the heat of decomposition should

not exceed 0.5 J/kg of wood (calculated using representative values of C_{pw} and T_p).

Flame Spread Rate

Figure 3 shows how the flame spread rate changes with the blowing parameter m and the charring constant c , whereas Fig. 4 shows how the velocity and mixture fraction profiles in the gas phase change with the blowing parameter m . Clearly, as m increases, both the flame (located at $Z = Z_0$) and the boundary layer move away from the burning surface. There are only a finite set of values of m for which the boundary layer solution exists with the maximum value of m being 1.239 before separation occurs [8]. This range is explored in Fig. 3, which shows that there is a large increase in the flame velocity as the value of the charring constant c , which defines the char-material interface, is decreased for the same value of m . For fixed values of c and m , the flame speed is seen to be directly proportional to U_∞ . This is also predicted by deRis's formula. Since small values of c result in higher flame speeds regardless of the blowing parameter, fire-safe materials should be designed to have large c values. These materials will form a thick char layer.

The overall graphic representation of the computed gas- and solid-phase solution is presented in Fig. 5. The calculated isotherms in wood and char (using the property values of Ref. [7]) are shown for

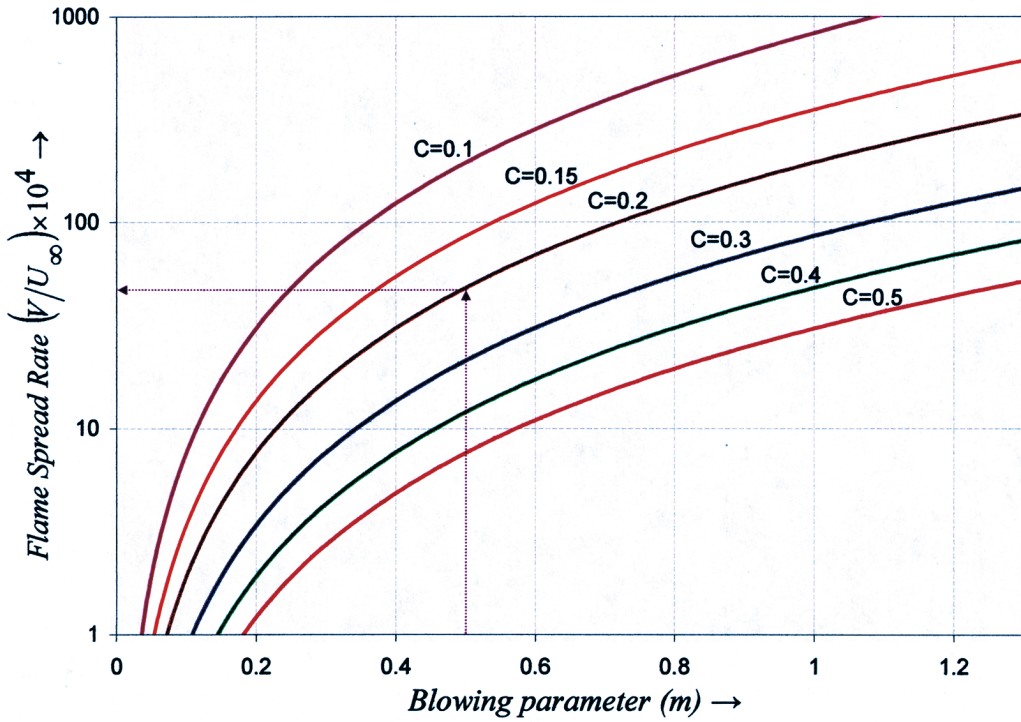


FIG. 3. A semilog plot of the variation of the flame spread velocity normalized by the free-stream velocity for various values of m and c . Boundary layer separation occurs for $m > 1.239$ [8].

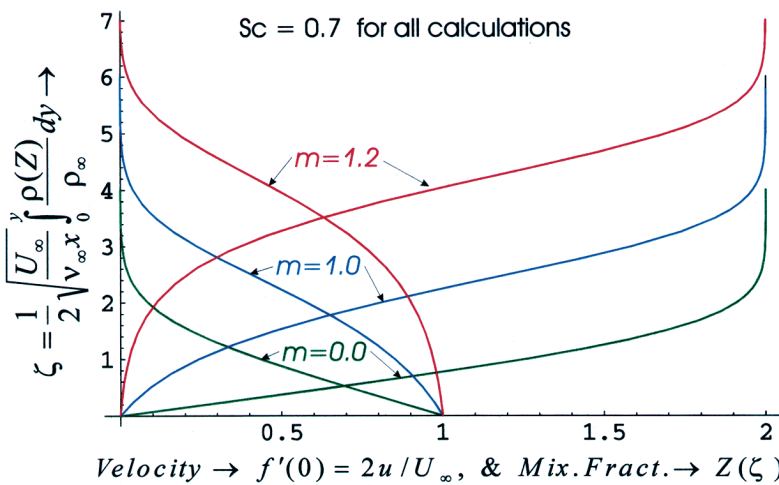


FIG. 4. Velocity and mixture fraction profiles inside the boundary layer. Boundary layer separation occurs for $m > 1.239$ [8].

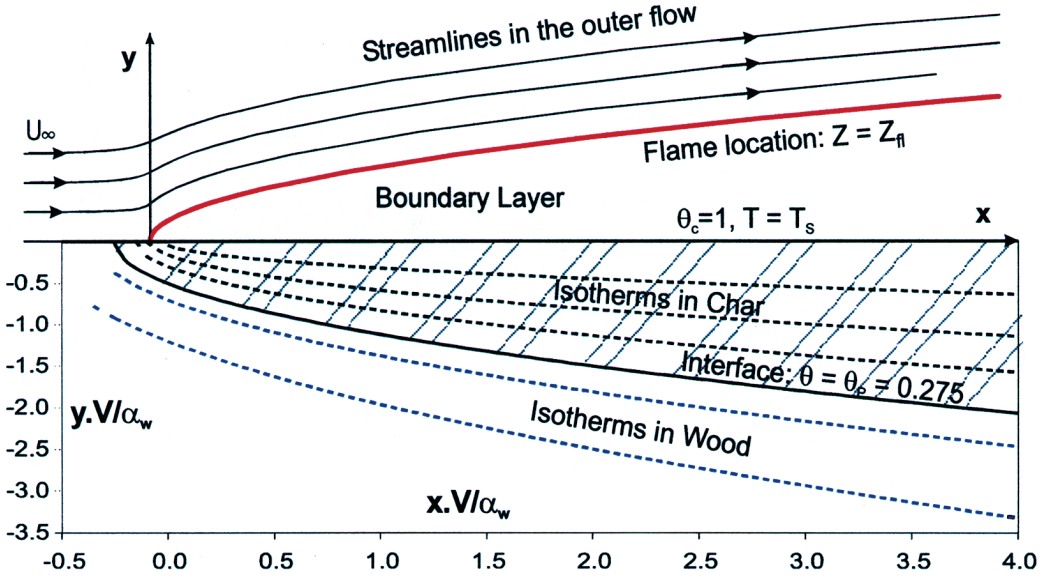


FIG. 5. Computed stream lines and the flame location in the gas phase along with the computed isotherms in wood and char. The property values used are from Ref. [7] for wood char.

$c = 0.501$, a value obtained by the graphical solution in Fig. 2. The corresponding calculations for the flame location and the stream lines in the gas phase are also shown. Upstream of the burning surface, the violation of the no-slip condition is evident from the stream lines for $x < 0$, whereas for $x > 0$, the stream lines diverge as expected. It is important to reiterate that this analysis, while not valid at the leading edge, solves fully elliptic nonlinear equations both in the solid and in the gas phase. The “thermal” part of the problem (i.e., the mass, energy, and species equations) is solved exactly. The only reason the gas-phase analysis is not an exact solution of the full Navier-Stokes equations is that the solution to the momentum equations breaks down locally for distances of the order of a few Stokes lengths downstream of the pyrolysis front and off the plate surface. This result is a generalization of deRis’s result [1] to charring materials with realistic gas flow. In the limit of a non-charring material (zero char thickness) and with Oseen approximation, it reduces exactly to deRis’s solution.

Comparison with Experiments

Experimental data for comparison with the model is not available in the configuration studied. This is because most investigators did not measure the char depth along with the flame spread rate. The available data is for axisymmetric fire spread on horizontal surfaces of wood [7]. For fire diameter greater than 5 cm, the flame spread may be approximated as two

dimensional along any radial direction. A comparison of this data with the model is presented in Fig. 6. The data are correlated according to the normalization used in the model, that is, $(Vy/\alpha_w)^2 = c^2 + 2c(Vx/\alpha_w)$. The value of α_w used for poplar wood is $0.1 \text{ mm}^2/\text{s}$, and (Vy/α_w) is plotted against (Vx/α_w) . For the data presented in Fig. 6, the actual measured flame velocity (which varied from 0.7 to 1.3 mm/s) for the four experiments was used. For the correlation, an average flame velocity for all the experiments (1 mm/s) was used. A good agreement between the data and the correlation implies that the measured flame spread rates and char depths follow the parabolic shape of the char-wood interface assumed in the model. The correlating equation also yields a value of the charring constant as $c \approx 0.2$ for poplar wood. Fig. 3 shows that for m ranging from 0.5 to 1 and $c = 0.2$, V/U_∞ varies from 0.005 to 0.02, implying that the induced air velocity (U_∞) must have been between 0.2 and 0.05 m/s. This is a reasonable estimate. The experiments and the model also show that smaller char depths are produced by higher flame speeds.

Nomenclature

- C_p specific heat at constant pressure [J/kg K]
- c charring constant defining the location of char-material interface[-]
- D mass diffusivity [m^2/s]

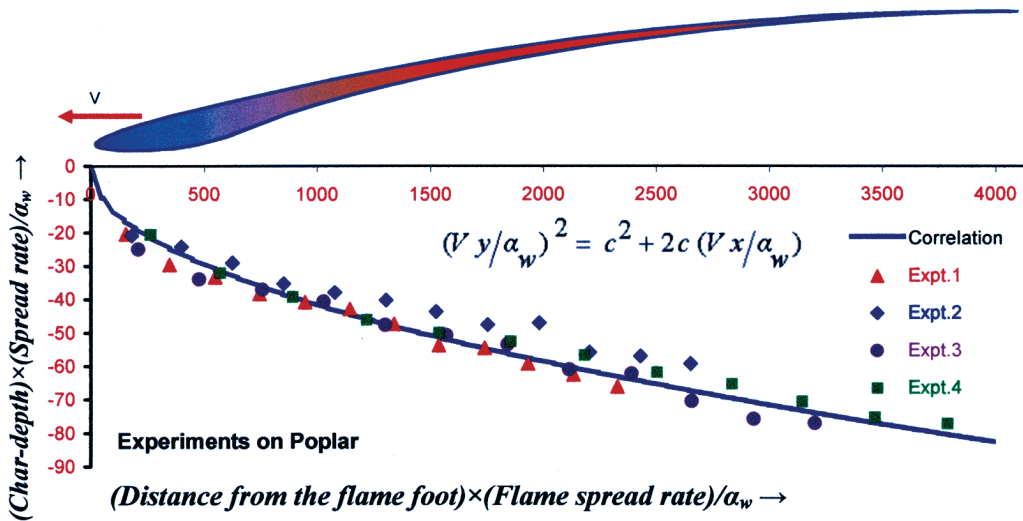


FIG. 6. Model correlation of experimental data from Atreya [7]. Measured flame spread rates and char depths are correlated according to the equation shown. Smaller char depths are produced by higher flame speeds.

f an arbitrary function defining the unknown isothermal boundary between char and pristine solid by $f(x, y) = \text{constant}$; also, solution of the Blasius flow problem

g an arbitrary function defining the unknown isothermal boundary between char and pristine solid by the equation $x = g(y)$

h^s the sensible enthalpy

m boundary layer blowing parameter

Q heat liberated or absorbed at the interface per unit mass of wood [J]

Q_O heat of reaction per unit mass of O_2 consumed

\bar{Q} Stefan number [-]

T temperature [K]

U free stream gas velocity in the flame-fixed coordinate system [m/s]

V steady flame spread velocity [m/s]

u, v gas velocities in the stream/wise and transverse directions describing the two-dimensional flow field

β, ω parabolic coordinates

x, y streamwise and transverse coordinates [m]

Y mass fraction

Z mixture fraction

Greek Symbols

α thermal diffusivity [m^2/s]

δ_c ratio of pristine solid to char thermal diffusivities [-]

λ thermal conductivity [W/mK]

$\bar{\lambda}$ ratio of char to pristine solid thermal conductivities [-]

ν kinematic viscosity [m^2/s]

ρ density [kg/m^3]

θ non-dimensional temperature

Subscripts

c char

F flame, fuel

g gas

p pyrolysis

w pristine solid (wood)

o oxygen

∞ values in the free stream

Acknowledgments

This paper is dedicated to the memory of Professor Howard W. Emmons and Professor George F. Carrier, who made immense contributions toward the education of the authors. The first author is grateful for financial support from NASA (contract no. NCC3-482) and NIST (grant no. 60NANB8D0080).

REFERENCES

- de Ris, J. N., *Proc. Combust. Inst.* 12:241–252 (1968).
- Fernandez-Pello, A. C., and Williams, F. A., *Combust. Flame* 28:251–273 (1977).
- Wichman, I. S., and Williams, F. A., *Combust. Sci. Technol.* 32:91–123 (1983).
- Quintiere, J. G., *Fire Mater.* 5:52–64 (1981).
- Atreya, A., in *Eighth International Heat Transfer Conference*, Hemisphere Publishing Corp., San Francisco, 1986, pp. 849–856.

6. Atreya, A., "Theory of Wind-Opposed Flame Spread over a Charring Solid," in *Proceedings of the Thirty-Fifth National Heat Transfer Conference*, ASME Press, Anaheim, CA, 2001.
7. Atreya, A., "Pyrolysis, Ignition and Fire Spread on Horizontal Surfaces of Wood," Ph.D. thesis, Harvard University, Cambridge, MA, 1983.
8. Emmons, H. W., *Z. Angew. Math. Mech.* 36:60–71 (1956).

COMMENTS

James Quintiere, University of Maryland, USA. In the deRis model [1], a simple thermal analysis can produce the solution, e.g., the flame speed, $v \approx \delta_f/t_{ig}$, where δ_f is the flame heating length and t_{ig} is the time to ignite the surface. The ignition time can be approximately given as $(k\rho c)_{solid}(T_f - T_{ig})$, with the flame heat flux approximated as $q'' \approx k_{gas}(T_f - T_{ig})/\delta_f$. The flame heating length can be represented as a diffusion length, $(k/\rho c)_{gas}/u_{gas}$, where u_{gas} is the gas velocity.

The flame temperature is proportional to $\Delta h_c - L_{effective}$, the net energy released per unit mass of the fuel. The effective heat of gasification contains the effect of char, and for a charring material, it is higher than that of a similarly non-charring material. Will this simple model explain your modified deRis solution?

REFERENCE

1. deRis, J. N., *Proc. Combust. Inst.* 12:241 (1968).

Author's Reply. Your physical analysis of flame spread is not different from the analysis presented in the paper. In the physical picture you outlined, essentially, the steady flame spread rate is obtained as a result of the balance established between the heat flux provided by the flame over a certain time (ignition delay time) and the ability of the solid to respond to this heat flux to produce fuel gases sufficient to support the flame. The primary difference is that you considered this balance only at the flame foot, whereas, in the similarity solution presented here, it is considered everywhere. For $y = 0$ and $x \geq 0$, that is, along the burning surface, the energy balance is satisfied by equation 28, and the gas-phase heat flux is utilized to produce fuel gases that yield the blowing parameter m according to equation 29 of the paper.

The difference between the flame foot and the global similarity analysis leads to a new way of thinking about flame spread. The flame, which is essentially a stoichiometric surface, moves upstream into the ambient air (flame spreads) as more fuel is produced by flame heat transfer to the solid. Thus, if we artificially heat the burning zone, by external radiation, everywhere except at and near the flame foot (characteristic dimension defined by $\delta_f \approx \delta_g \approx \alpha_g/U_g$, as you identified), the flame spread rate will increase according to the similarity analysis (because m will increase; Fig. 3), but it will remain unaltered according to the flame foot analysis. If such an experiment is conducted, we believe that it will show an increase in the flame-spread rate.

It is also important to emphasize that upstream diffusion of energy and species in the gas phase is fully considered in the model, since fully elliptic equations are solved. Thus, both heat and mass diffuse upstream into the oncoming ambient air, resulting in flame spread. Simultaneously, heat also diffuses upstream into the solid to produce fuel. As more fuel is produced, the flame moves upstream to accommodate it, and flame spread is said to occur.

The treatment of charring materials by using an effective heat of gasification, L_{eff} , may be approximately possible. Using deRis's assumptions, we obtain equation 32, which contains the charring factor $erf(\sqrt{\delta_c/2c}/(T_s - T_p))$. In the limit of zero char thickness ($c \rightarrow 0$ and $T_p \rightarrow T_s$), this factor reduces to $\sqrt{\lambda_c \rho_c C_{pc}}/\sqrt{\lambda_w \rho_w C_{pw}}(T_s - T_\infty)$, and equation 32 reduces to deRis's flame spread formula. For a charring material, the charring factor may be considered as modifying the flame temperature term ($T_f - T_s$), and thus a L_{eff} may be identified. However, the thermal inertia of char instead of the virgin material must be used.

Jay Gore, Purdue University, USA. Can the locations of the charring front and the flame front leading edges be separated from each other, as they appeared to be in the experiments you showed?

Author's Reply. We have never observed the location of the flame front or the charring front separated from each other, and they should not be because charring results in the production of fuel that supports the flame. There are three reasons why the experimental photographs look as they do. First, they were not taken edgewise to observe the flame foot. Second, the less luminous blue flame front is not visible in the predominantly luminous yellow flame. Third, the photographs image a much larger area compared to the flame foot; thus, resolution at the flame foot is poor.

Carlos Fernandez-Pello, University of California, Berkeley, USA. Could the transient aspects of flame spread in charring materials often observed be incorporated in your model through the parameter c , or can your model only account for the growth of the charring layer?

Author's Reply. The model is for steady-state flame spread over charring materials. It solves the nonlinear equations for the unknown parabolic char-material interface defined by the parameter c . We do not believe that it is possible to account for transient aspects through the parameter c in this model.